J Mater Sci: Mater Electron (2016) 27:6502–6510
DOI 10.1007/s10854-016-4592-4

Effect of laser irradiation on activation energy, irreversibility field and upper critical magnetic field of bulk MgB_2 superconductor

O. Erdem[1,2] · E. Yanmaz[2]

Received: 27 October 2015 / Accepted: 26 February 2016 / Published online: 1 March 2016
© Springer Science+Business Media New York 2016

Abstract In this study, the role of laser irradiation on the upper critical field (H_{c2}), the irreversibility field (H_{irr}) and the activation energy (U_0) of bulk MgB_2 superconductor was first time investigated with the aid of magnetoresistivity measurements conducted at different applied magnetic fields in a range of 0–15 kOe as a function of temperature from 25 to 40 K. For this aim, a disk shaped MgB_2 superconductor was produced and cut into two pieces. One of the pieces was irradiated under high vacuum conditions by using an Nd:YVO_4 laser. The obtained results showed an increase in the critical temperature (T_c) by about 1 K after irradiation. Also, the values of $H_{c2}(0)$ were respectively found to be around 143 and 151 kOe while the values of $H_{irr}(0)$ were about 122 and 130 kOe for the reference and the irradiated samples. Using the thermally activated flux flow model the dependence of U_0 on magnetic field was determined. The maximum U_0 values of 0.43 and 0.83 eV in zero magnetic field were respectively obtained for the reference and the irradiated samples. Also, the magnetic field dependence of the critical current density $J_c(B)$ values at different temperatures were slightly increased after the irradiation. These results point out that the superconducting properties of bulk MgB_2 can be improved via laser irradiation.

✉ O. Erdem
ozgemerdem@hotmail.com; ozgeerdem@bayburt.edu.tr

[1] Department of Medical Services and Techniques, Bayburt Vocational High School of Health Services, Bayburt University, 69000 Bayburt, Turkey

[2] Department of Mechatronics, Faculty of Engineering and Architecture, İstanbul Gelişim University, 34310 Istanbul, Turkey

1 Introduction

MgB_2 superconductor discovered by Nagamatsu et al. [1] in January 2001 is an attractive candidate for practical applications at around 20 K because of its excellent superconducting properties such as its simple chemical composition, low material cost, simple crystal structure, high transition temperature ($T_c = 39$ K) [1] among the intermetallic superconductors, high upper critical field [2, 3] (20–240 kOe for $H_{c2}^{//c}$ (0) and 140–390 kOe for $H_{c2}^{//ab}$ (0) [4]) high critical current density (J_c) [5, 6] (J_c (4.2 K, 0 T) $> 10^7$ Acm^{-2} [4]), and the absence of weak links [7].

The quality of a superconductor is considerably important for technological and engineering applications. Therefore, almost all research groups focus on the improvement of superconducting properties and flux pinning performance of MgB_2 material in the forms of polycrystalline bulk, wire, tape and thin film. As well known, the dramatic fall of critical current density in an external magnetic field due to the insufficient pinning centres and the rapid decrement of the flux pinning energy in the bulk MgB_2 limit the potential applications in technology and industry of the MgB_2 material at high magnetic fields. In literature, various studies include of different methods such as adding or doping [8, 9], mechanical alloying [10], hot isostatic press [11] etc. have been carried out with the goal of improving the pinning performance of MgB_2. One of the promising methods for enhancing the superconducting properties of MgB_2 is the introduction of defects and atomic disorders by means of particle irradiation. The energetic particles passing through the sample perturb the crystal lattice and induce effective pinning centres such as point-like defects, cluster defects and columnar defects which improve the pinning of vortices resulting in the increment of the critical current density of the MgB_2 material [12–15].

The study reported by Shinde et al. [12] showed only marginal enhancement in J_c for the irradiated MgB_2 films by 200 MeV Ag ions because of the cluster defects. Additionally, in the heavy-ion irradiated MgB_2 samples the irreversibility field shifted to higher field regions with no enhancement in J_c at the lower field region because of the induced columnar defects [13]. The study of gamma-rays irradiation on bulk MgB_2 samples, reported by Obaidat et al. [15], showed an enhancement in critical current density because of the migration of MgO inside the MgB_2 grains which improves grain connectivity and causes oxygen related defects in grains and also oxygen segregation in grain boundaries where it increases the vortex flux pinning.

As known from literature, the flux motion related to the pinning energy has a role to keep the magnetic flux in the pinning centres as a potential energy barrier and over the pinning energy barrier of a superconductor, the flux line might be thermally activated although the Lorentz force is smaller compared to the pinning force. The thermally activated flux flow (TAFF) model works well in the low resistivity region near T_c ($\rho = 0$) of a superconductor [16–20]. Moreover, the flux pinning force density and the activation energy give an explicit inside into the flux pinning ability of a superconductor due to the fact that the pinning energy is generally regarded as a measure of flux pinning strength of a superconductor material [21–23]. Thus, it is crucial to study the activation energy against flux motion to understand the pinning mechanism and to enhance the current carrying capacity of a superconductor. The activation energy determined from the TAFF model can be described by Arrhenius equation given below

$$\rho(T,H) = \rho_0 \exp(-U_0/k_B T) \quad (1)$$

where $\rho(T, H)$ is the resistivity value of the samples at the temperature of T and in magnetic field of H, ρ_0 is the preexponential factor independent of field, k_B is the Boltzmann constant and U_0 is the flux-flow activation energy.

In the present work, the resistive transitions of laser-irradiated and unirradiated MgB_2 bulk samples were conducted up to 15 kOe in a range from 25 to 40 K. The critical temperatures (both the onset and the offset), irreversibility fields and upper critical fields were evaluated from the magnetoresistivity curves. At the same time, magnetic field and temperature dependence of the activation (flux pinning) energies of both samples were determined with the aid of thermally activated flux flow (TAFF) model. Also, the critical current densities at different temperatures ($T = 5$, 10 and 15 K) of the samples were analysed with magnetic measurements. The results obtained from this study examining the superconductor-laser beam interaction have shown the T_c enhancement as the first bullet point and the improvement of superconducting properties (H_{c2}, H_{irr} and J_c) for the laser irradiated bulk MgB_2 sample. Also, this study is an important source to give information for vortex dynamics and flux pinning phenomena of a laser irradiated MgB_2 superconductor.

2 Experimental details

For this study, a disk-shaped MgB_2 superconductor was produced from commercially available high purity powders of Mg (−325 mesh, 99.8 %, Alfa Aesar) and amorphous nano B (>98 %, Pavezyum) by using hot press method at 200 °C and followed by pellet/closed tube method at 650 °C for 3 h. The bulk MgB_2 in this study was produced by using the same production condition described in our previous study [24]. The obtained bulk sample with 18.5 mm in diameter and 2.5 mm in height was cut into two parts. These parts were named as 650R and 650L. The hot pressed surface of the sample 650L was irradiated by Nd:YVO_4 laser (Powerline E, Rofin) working on continuous mode and emitting at a wavelength of 1064 nm in combination with a vacuum chamber coupled to an automatized positioning system to perform the laser scanning treatment of the samples. The sample 650R was considered as reference one.

The experimental set-up employed in this study was shown in Fig. 1. The laser apparatus, which allows scanning the surface of the samples within the xy-plane, was fitted with a galvanometer beam steering system and a flat-field lens with a 160 mm focus. In order to apply the laser irradiation, the sample 650L was firstly placed into the vacuum chamber. At a high vacuum condition (around 10^{-6} mbar), a laser scanning process was applied to this sample displaced at 0.08 mm/s in ±x direction. The laser beam was set to scan the surface of the sample on the ±y direction with an irradiance of 8.63×10^6 Wcm^{-2} in continuous mode. The laser irradiation scanned the surface at 500 mm/s during the motion in ±y direction.

The phase compositions of the samples were studied by X-Ray Diffraction (XRD) with a Rigaku D/Max-IIIC X-ray diffractometer. The X-rays were normally generated at 40 kV and 30 mA. Measurements were performed at 2θ between 20° and 80° with step = 0.03° and $t = 2$ step/m. Also, the effect of laser irradiation on the surface morphology of the samples was analysed with a Carl Zeiss MERLIN™ field-emission scanning electron microscope (FESEM) at different magnifications.

The magnetoresistivity measurements as a function of temperature $\rho(\mu_0 H, T)$ in the applied magnetic field ranging of 0–15 kOe were carried out by the standard d.c. four-probe technique using He cryostat system from 40 K down to 25 K at constant driving current of 10 mA. The

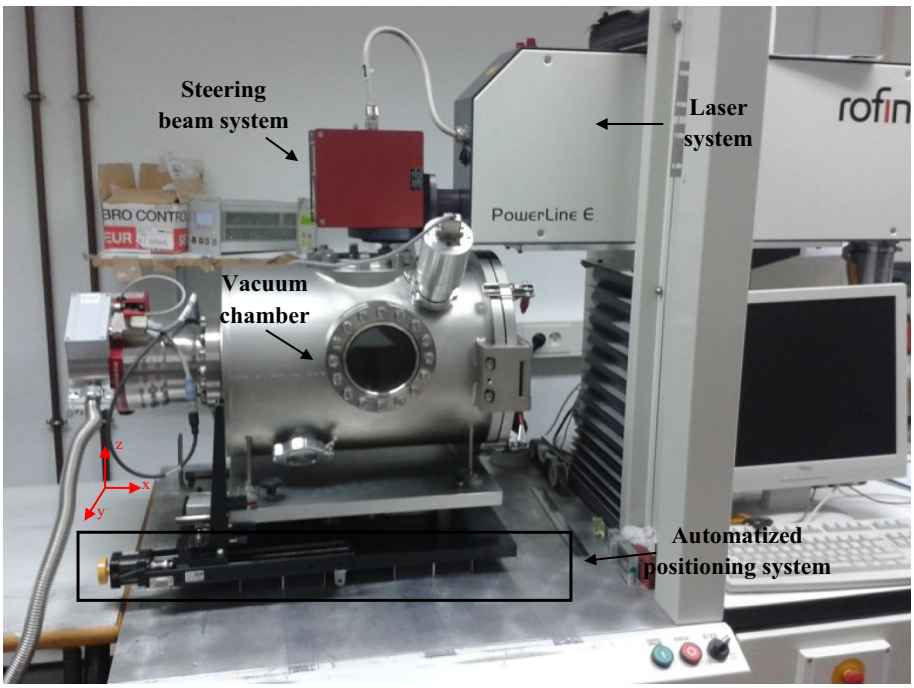

Fig. 1 The experimental setup used for the laser irradiation in this study

magnetic fields generated from the superconducting coil magnet were applied parallel to the hot pressing direction. It means the applied magnetic field was normal to the irradiated surface of the sample 650L. The measurements were performed after zero field cooling (ZFC) of the samples providing the absence of a remanent magnetization. Furthermore, the onset ($T_{c,\text{onset}}$) and offset ($T_{c,\text{offset}}$) critical temperatures of the samples, cut for resistivity measurements in appropriate dimensions, were inferred from the magnetoresistivity curves and the activation energy (U_0) values were determined by means of the thermally activated flux flow (TAFF) model, which calculates the flux pinning energy by making linear fits to the low resistivity part of the transition [25–27]. From the magnetoresistivity curves some theoretical results such as the irreversibility field (H_{irr}) and the upper critical field (H_{c2}) were also computed for both samples. At constant applied magnetic field the temperature dependent resistance can be written as [28, 29].

$$R(\mu_0 H_{\text{irr}}, T) = 0.1R_n \text{for the } \mu_0 H_{\text{irr}}(T) \text{ and } R(\mu_0 H_{c2}, T) = 0.9R_n \text{ for the } \mu_0 H_{c2}(T) \quad (2)$$

where R_n denotes the normal state resistivity of the samples at 40 K and 0 kOe. The intercepts of linear extrapolation of $\mu_0 H_{c2}(T)$ and $\mu_0 H_{\text{irr}}(T)$ to zero on the temperature axis are taken as the direct $\mu_0 H_{c2}(0)$ and $\mu_0 H_{\text{irr}}(0)$ respectively [30].

The magnetic hysteresis M(H) of both samples were obtained using a Vibrating Sample Magnetometer (VSM) attached on the Physical Properties Measurement system (PPMS, Quantum Design), in a magnetic field up to ±7 T with a sweep rate of 100 Oe/s at three different temperatures of 5, 10 and 15 K. The M(H) loops were measured with the magnetic field applied perpendicular to the pressed surface (the pressed surface was also normal to the beam direction). The $J_c(B)$ ($B = \mu_0 H$) dependence of the samples was calculated by using the equation $J_c = 20\Delta M/[a(1-a/3b)]$ based on Bean's critical state model [31]. In this relationship, ΔM is the difference between upper and lower branches of the M(H) curve (in emu) divided by the volume of a sample (in cm^3), a × b is the surface area of a sample which is perpendicular to the direction of the applied magnetic field with b > a, a and b are in cm, while J_c is in Acm^{-2}.

3 Results and discussions

The phase compositions of the reference and the irradiated samples are shown in Fig. 2a, b, respectively. The X-ray patterns of the 650R and 650L samples show almost same phase structures. The analysis shows the lack of alignment between the MgB_2 grains and the presence of impurities (some residual unreacted Mg and MgO), as seen from Fig. 2. The presence of MgO phase is possibly due to the entrapped air in the chrome tube during end-sealing step. Peaks associated to MgB_4 or other higher borides are not observed in the samples, confirming that there was not any evaporation of Mg during heat treatment and laser irradiation process. From these results one can say that the MgB_2

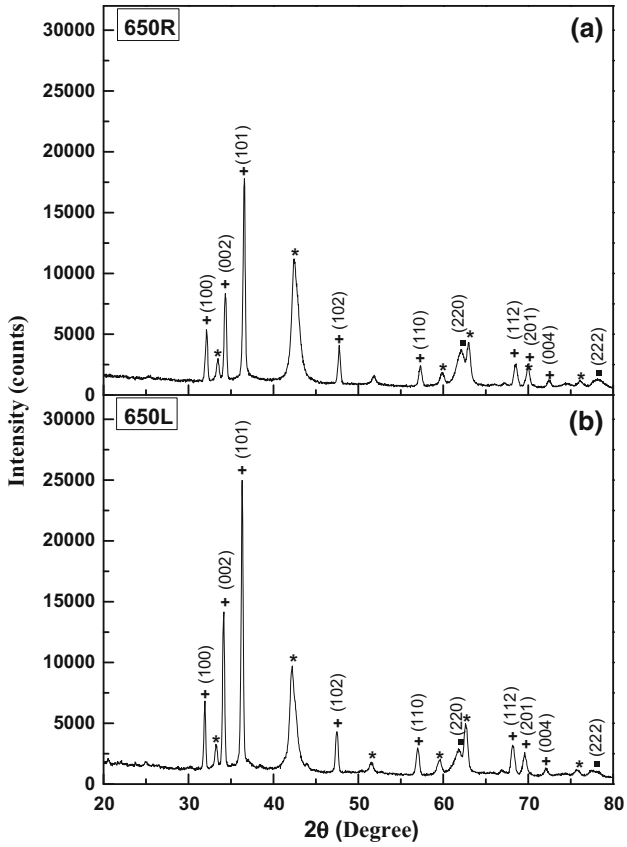

Fig. 2 XRD diffraction patterns of **a** the 650R sample and **b** the 650L sample. MgB_2, Mg and MgO phases are shown with the symbols of *asterisk*, *plus* and *square*, respectively

phase is preserved in the partially melted sample during the irradiation.

The morphological changes induced by the laser irradiation on the surface of the irradiated sample 650L were examined using FESEM. Figure 3a–d show the FESEM images of the 650R and 650L samples, respectively. Comparing Fig. 3a, c, it can be said that the laser irradiation promotes a melting and a subsequent ejection process on the surface of the irradiated sample because of the energy transferred to the surface of the sample during irradiation process. In addition, comparing Fig. 3b, d, it can be said that the grains are significantly grown due to the laser-induced sintering, which improves the interconnectivity among the superconducting grains [32]. Okutomi et al. [33] and Roul et al. [32] also reported the grain growth after the irradiation for $YBa_xSr_{2-x}Cu_3O_{7-y}$ and $SmBa_2Cu_3O_x$ high T_c superconductors, respectively. The modified surface appears dense and compacted grains, uniform grain size distribution and better crystallinity, since many pores exist among grain boundaries in the unirradiated sample. Also, the average grain size of the 650R sample is under 0.1 μm and for the 650L sample it is about 0.2–0.8 μm.

Figure 4a, b show the temperature dependence of the normalized resistance $\rho_{T,H}/\rho_{40\ K,\ 0\ kOe}$ as a function of applied magnetic field up to 15 kOe for the irradiated sample 650L and the reference sample 650R, respectively. It can be seen from Fig. 4 that the superconducting transition is sharper for the sample 650L than that of the reference one. The transition temperature values ($T_{c,\text{onset}}$ and $T_{c,\text{offset}}$) of both samples were obtained using the criteria of 90 and 10 % of the normalized resistivity curves in different magnetic fields. Additionally, the transition range (ΔT_c) was determined from the difference between the values of $T_{c,\text{onset}}$ and $T_{c,\text{offset}}$. Table 1 shows the variation of the transition temperatures deduced from Fig. 4 for both samples. One can see from this table that the $T_{c,\text{onset}}$ and $T_{c,\text{offset}}$ values are suppressed to the lower temperatures with the enhancement of applied magnetic field because of the reduction of pinning force in the system [34] and the thermally activated flux flow (TAFF) of vortices [35]. It is known that the $T_{c,\text{onset}}$ is related to the transition of isolated grains to the superconducting state and the $T_{c,\text{offset}}$ is accordance with the features of inter-granular component [36]. The maximum $T_{c,\text{onset}}$ of 35.8 and 37.1 K and the maximum $T_{c,\text{offset}}$ of 34.4 and 36.5 K were observed for the reference and the irradiated samples at zero magnetic field. At 15 kOe applied field, the $T_{c,\text{onset}}$ values decreased to 32.1 and 33.4 K, also the $T_{c,\text{offset}}$ values decreased to 30.2 and 32.2 K for the reference and the irradiated samples. From these results, it can be seen that the T_c values increase by about 1 K and the strong field dependence of the critical temperature decreases after laser irradiation. It indicates enhancing interconnectivity between grains [37] and reduction of porosity, as consistent with the FESEM image (see Fig. 3d). Moreover, it is known that the broadening tail part ($R \approx 0$) of the magnetoresistivity curves shifts to lower temperature with increasing applied magnetic field as a result of the decrement in the flux pinning ability of the superconducting samples [38]. So, the variation of ΔT_c values at different applied magnetic fields gives important results. It can be seen from Table 1 that the maximum ΔT_c of 1.9 K is observed for the sample 650R at 15 kOe while the variation is found to be 1.2 K for the sample 650L, illustrating that the latter exhibits stronger pinning ability compared to the other one [34].

Upper critical magnetic field ($H_{c2}(T)$) and magnetic irreversibility field ($H_{\text{irr}}(T)$) are the important parameters to characterize the pinning ability of superconductors. So, $H_{c2}(T)$ and $H_{\text{irr}}(T)$ values at various temperatures of the reference and the irradiated samples were respectively determined using the criteria of 90 and 10 % of normalized resistivity curves shown in Fig. 4. The curves of $H_{c2}(T)$ and $H_{\text{irr}}(T)$ are illustrated in Fig. 5a, b, respectively. It is apparent from the Fig. 5 that the $H_{c2}(T)$ and $H_{\text{irr}}(T)$ curves of the sample 650L expands to higher temperature

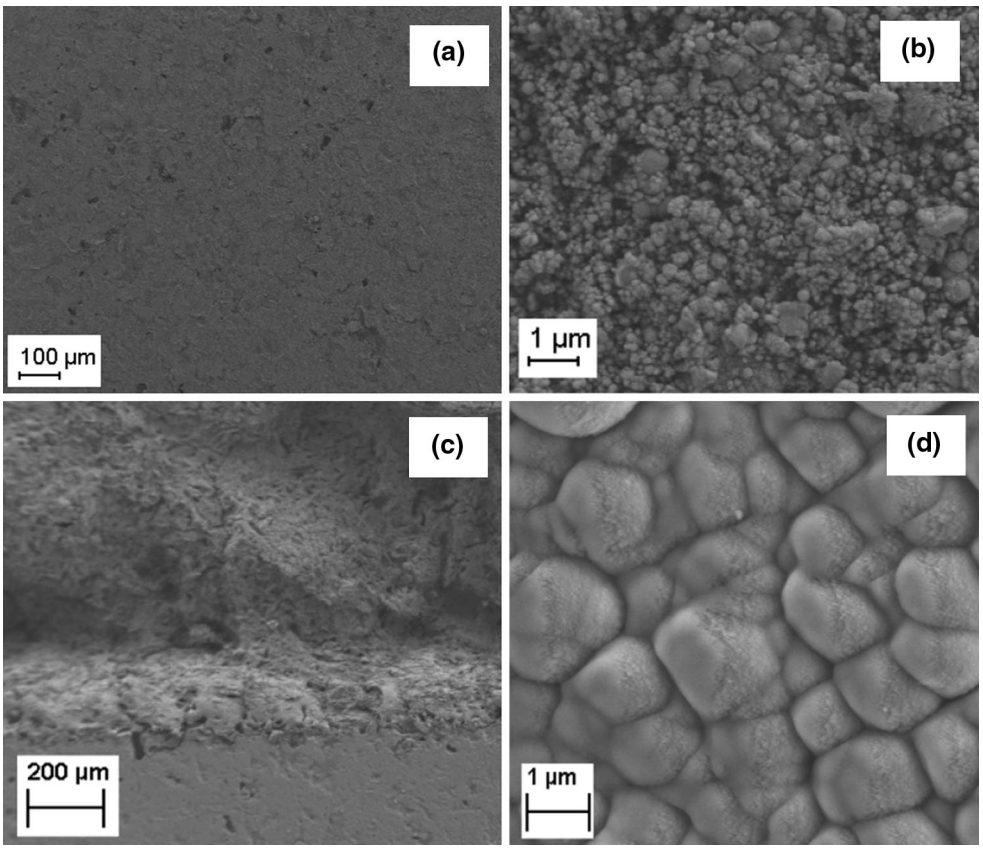

Fig. 3 FESEM images of **a**, **b** the 650R sample and **c**, **d** the modified surface by continuous mode laser irradiation of the 650L sample at different magnifications

indicating an enhancement in the strength of the flux pinning [34, 37]. Additionally, the values of $H_{c2}(0)$ and $H_{irr}(0)$ at $T = 0$ K were calculated by the linear extrapolation of the curves shown in Fig. 5a, b to the absolute zero temperature ($T = 0$ K) for both samples. The $H_{c2}(0)$ and $H_{irr}(0)$ were respectively obtained as 143 and 122 kOe for the sample 650R and 151 and 130 kOe for the sample 650L. It was reported that the values of $H_{c2}^{//c}(0)$, $H_{c2}^{//ab}$ and $H_{irr}(0)$ of MgB_2 superconductor are 20–240, 140–390 and 60–350 kOe, respectively [4]. The obtained values are compatible with the literature. Furthermore, the ratio between the $H_{c2}(0)$ and $H_{irr}(0)$ values gives a clue about the pinning properties of a superconductor. These ratios are 0.853 and 0.861 for the sample 650R and the sample 650L, pointing well agreement with the previously reports for MgB_2 superconductors [20, 38, 39]. Based on this result, the ratio slightly enhances after the laser irradiation.

Because of the barrier value of the activation (flux pinning) energy depends on the temperature and the magnetic field, Arrhenius activation law can be used to determine the pinning energy of a superconductor in the low resistivity region. According to Eq. (3) given below and derived from Eq. (1), the activation energy at different applied magnetic fields can be estimated from the slope of the linear part in broadening tails of the Arrhenius graphs [40, 41].

$$U_0 = -k_B T \ln\left(\frac{\rho}{\rho_0}\right) \tag{3}$$

In order to understand the laser irradiation effect on the flux flow of bulk MgB_2 material, the Arrhenius plots of ln ($\rho_{T,H}/\rho_{40\ K,\ 0\ kOe}$) versus $1/T$ obtained from Fig. 4 were plotted for both samples and shown in Fig. 6. The linear parts in each ln ($\rho_{T,H}/\rho_{40\ K,\ 0\ kOe}$) versus $1/T$ curves shown in Fig. 6, represent the energy dissipation due to the thermal activation of flux across the pinning barrier [42].

Figure 7 shows the variations of activation energies of the sample 650R and the sample 650L with increasing magnetic field applied parallel to the pressing direction of both samples. One can see from Fig. 7 that the pinning energy depends on the applied magnetic field. The activation energy of the reference sample 650R is about 0.29 eV at 10 kOe as shown in Fig. 7. This value is consistent with the literature [43, 44]. Also, it can be seen that the activation energy values are higher for the sample 650L in existence of magnetic field than that of the sample 650R.

Therefore, flux lines are pinned strongly against the Lorentz force in the laser-irradiated sample [45]. The maximum activation energy values for the reference and the irradiated samples are approximately 0.43 and 0.83 eV in zero magnetic field, respectively. At 15 kOe applied magnetic field, these values are respectively found to decrease to 0.24 and 0.48 eV, confirming the shortening of the distance between pinning centres and the decrement of the energy barriers in the samples studied [46]. These results reflect the strong pinning effect of the vortices and enhancement of the vortex pining force in the sample 650L.

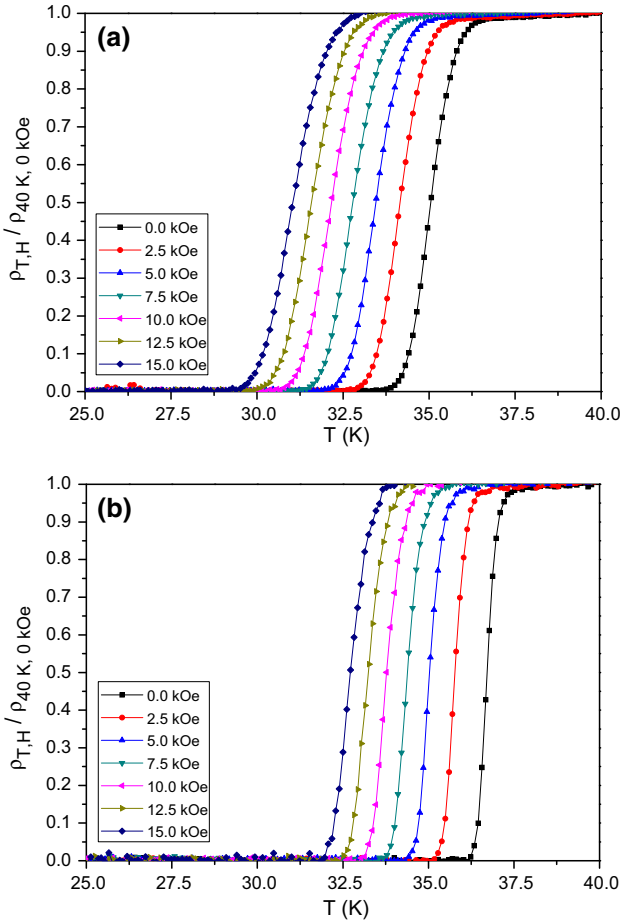

Fig. 4 Temperature dependence of the normalized resistance of **a** the reference sample 650R and **b** the irradiated sample 650L in different applied magnetic fields

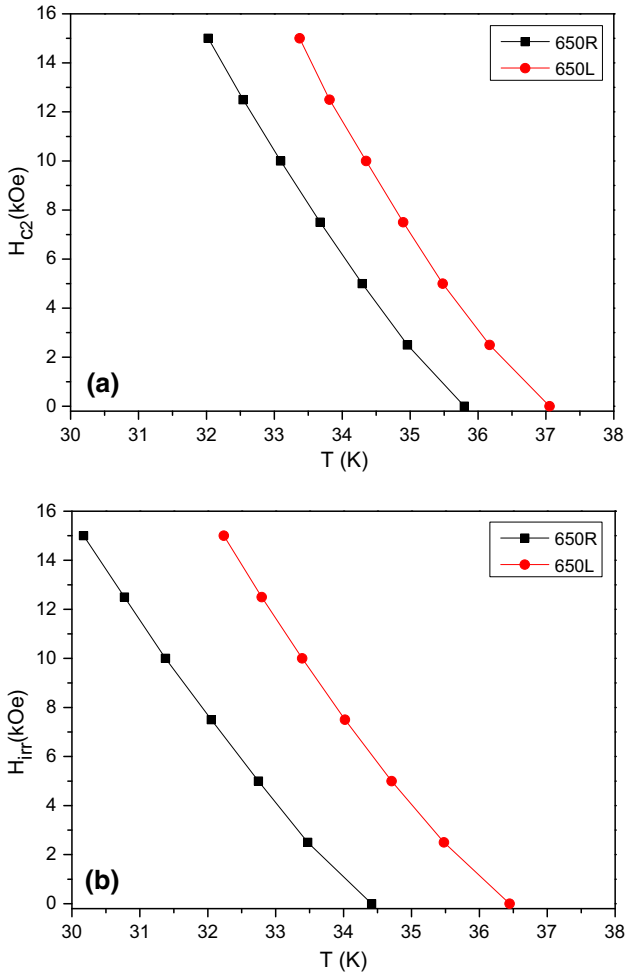

Fig. 5 The upper critical field (H_{c2}) and the irreversibility field (H_{irr}) as a function of temperature for **a** the reference sample 650R and **b** the irradiated sample 650L

Table 1 The $T_{c,onset}$, $T_{c,offset}$ and ΔT_c values obtained from Fig. 4 for the reference sample 650R and the irradiated sample 650L

Sample 650R	0.0 kOe	2.5 kOe	5.0 kOe	7.5 kOe	10.0 kOe	12.5 kOe	15.0 kOe
$T_{c,onset}$ (K)	35.8	35.0	34.3	33.7	33.1	32.6	32.1
$T_{c,offset}$ (K)	34.4	33.5	32.7	32.1	31.4	30.8	30.2
ΔT_c (K)	1. 4	1.5	1.6	1.6	1.7	1.8	1.9
Sample 650L	0.0 kOe	2.5 kOe	5.0 kOe	7.5 kOe	10.0 kOe	12.5 kOe	15.0 kOe
$T_{c,onset}$ (K)	37.1	36.2	35.5	34.9	34.3	33.8	33.4
$T_{c,offset}$ (K)	36.5	35.5	34.7	34.0	33.4	32.8	32.2
ΔT_c (K)	0.6	0.7	0.8	0.9	0.9	1.0	1.2

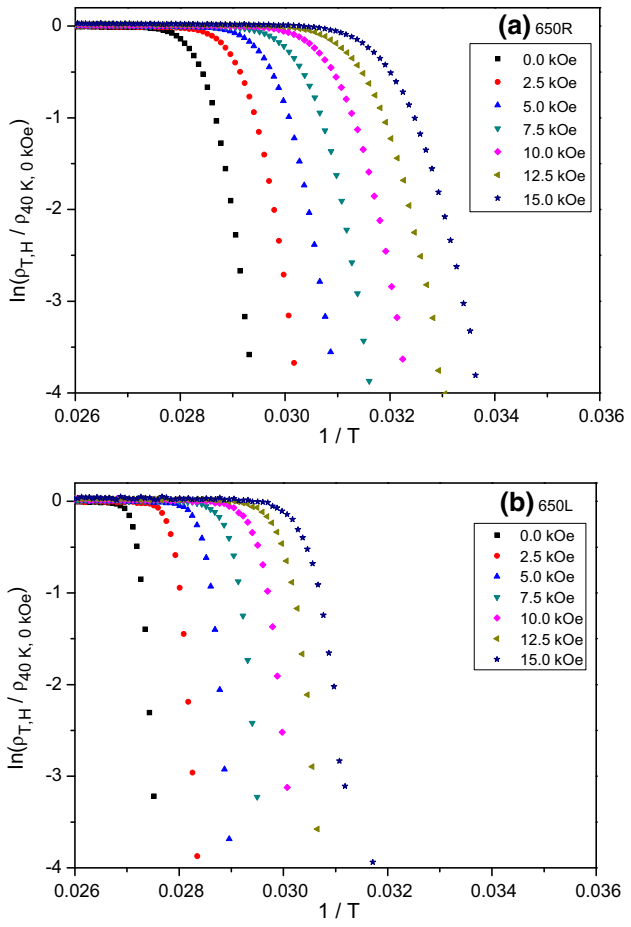

Fig. 6 Arrhenius plots of the normalized resistance for **a** the reference sample 650R and **b** the irradiated sample 650L at different applied magnetic fields

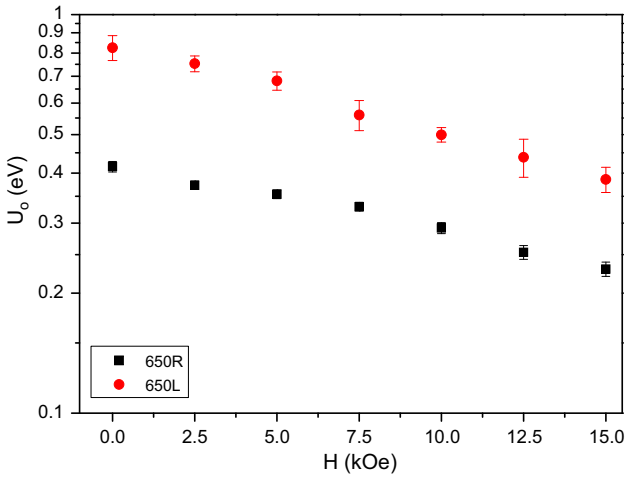

Fig. 7 Magnetic field dependence of the flux-flow activation energy, U_0, for the reference sample 650R and the irradiated sample 650L

Figure 8 shows the magnetic field dependence of critical current densities $J_c(B)$ of the reference and the irradiated samples at different temperatures of 5, 10 and 15 K. It is known that the J_c obtained from magnetic hysteresis loops determines the critical properties of the individual grains, i.e., the intra-granular current [45]. The J_c values calculated from the width of magnetic hysteresis loops shown as inset

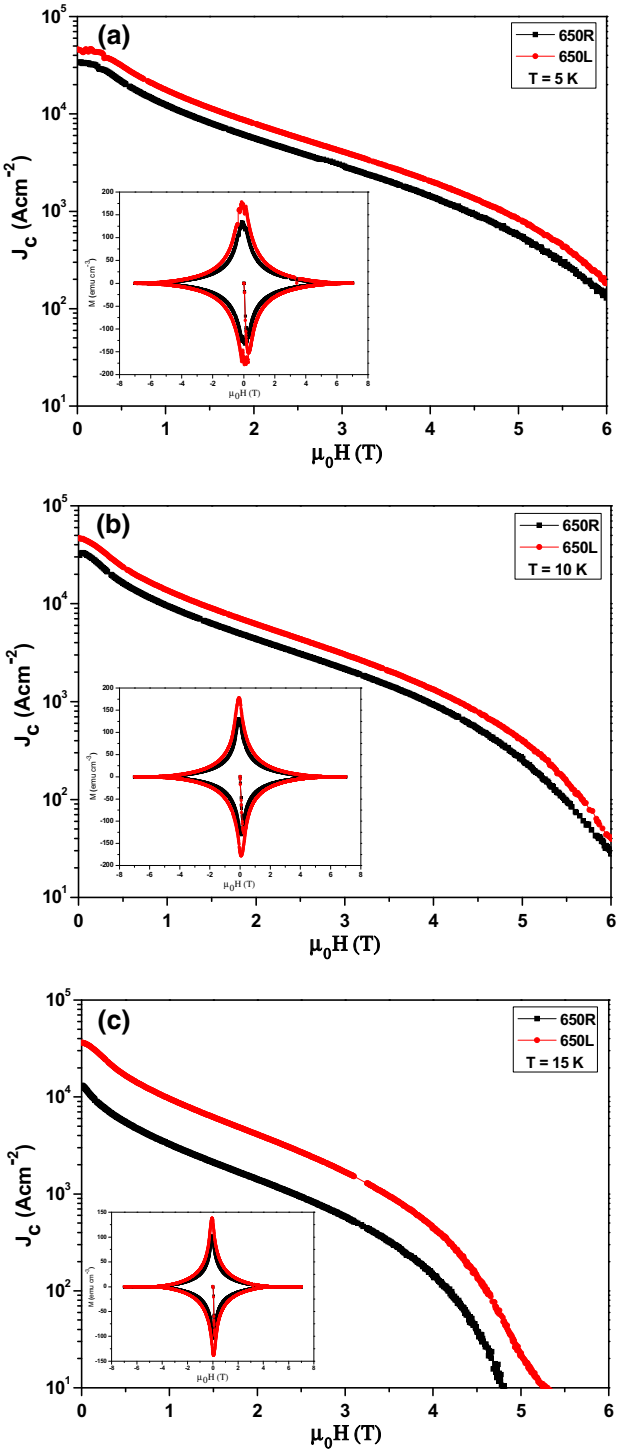

Fig. 8 Magnetic field dependence of critical current density J_c(-B) curves of the samples 650R and 650L at **a** 5 K, **b** 10 K and **c**15 K. The *inset* figures show the magnetization versus magnetic field curves at different temperatures for the corresponding samples

Table 2 The J_c values of the reference sample 650R and the irradiated sample 650L

	650R	650L
J_c (5 K, 3 T) (Acm^{-2})	2.96×10^3	4.10×10^3
J_c (10 K, 3 T) (Acm^{-2})	2.15×10^3	3.03×10^3
J_c (15 K, 3 T) (Acm^{-2})	5.74×10^2	1.67×10^3

figures in Fig. 8, are given in Table 2 for 3 T at the temperatures of 5, 10 and 15 K. Considering the effect of laser irradiation on the critical current density, the 650L sample shows higher J_c in an external field at all measurement temperatures, especially at 15 K, as compared with the 650R sample, consistent with the computed U_0 energies. The J_c values were calculated as 2.96×10^3 and 4.10×10^3 Acm^{-2} at 5 K and 3 T for the reference and the irradiated samples, respectively. The enhancement of J_c values at high magnetic fields is maybe due to the creation of additional defects induced by laser irradiation, which act as pinning centres [32]. Note that the magnetization current results from the flux within the grains for sintered samples in the superconducting mixed state of a type-II superconductor [45]. From these results, it can be said that the laser irradiation enhances the flux pinning capability and pinning force of MgB_2.

4 Conclusions

In this study, we have presented the effect of laser irradiation on some superconducting properties such as critical temperature, irreversibility field and upper critical field of the bulk MgB_2 superconductor via the magnetoresistivity measurements conducted in a range of 0–15 kOe applied magnetic fields. The flux pinning (activation) energies at different applied magnetic fields and the critical current densities at different measurement temperatures for the studied samples were also evaluated from Arrhenius plots by using TAFF model and magnetic measurements, respectively. Also, some structural and morphological changes were presented. The findings were summarized below:

- The phase composition did not change after the laser irradiation. It shows the MgB_2 phase is preserved in the partially melted sample during the irradiation.
- The grains of the irradiated sample were significantly grown due to the laser-induced sintering. The modified surface appeared dense and compacted grains, uniform grain size distribution and better crystallinity, since many pores exist among grain boundaries in the unirradiated sample. These results imply the interconnectivity among the superconducting grains improves after irradiation.
- The critical temperature values enhanced by about 1 K after the laser irradiation. The $T_{c,\text{onset}}$ and $T_{c,\text{offset}}$ values were observed to be about 35.8 and 34.4 K for the reference sample whereas the maximum ones were obtained to be 37.1 and 36.5 K for the irradiated sample at zero magnetic field, respectively. The $T_{c,\text{onset}}$ and $T_{c,\text{offset}}$ values of the reference sample reduced to 32.1 and 30.2 K at 15 kOe applied magnetic field while the $T_{c,\text{onset}}$ and $T_{c,\text{offset}}$ values of 33.4 and 32.2 K were found for the irradiated sample, respectively. These increments in T_c values demonstrates the improvement of interconnectivity between grains, consistent with morphological changes in the irradiated sample.
- The irreversibility field and the upper critical magnetic field increased after the irradiation because of the enhancement of the flux pinning mechanism in the irradiated sample. The $H_{c2}(0)$ and $H_{\text{irr}}(0)$ values were 151 kOe (143 kOe) and 130 kOe (122 kOe) for the irradiated (the reference) sample.
- The irradiated sample showed higher U_0 values as compared with the reference one in the presence of applied magnetic field. It illustrates that the irradiated sample has stronger vortex pinning force and so, can carry current with minimum energy dissipation in the existence of applied magnetic field.
- The irradiated sample showed higher J_c in an external field at all measurement temperatures, especially at 15 K, as compared with the reference one, consistent with the computed U_0 energies. The J_c values were calculated as 2.96×10^3 and 4.10×10^3 Acm^{-2} at 5 K and 3 T for the reference and the irradiated samples, respectively. These results show that the laser irradiation enhances the flux pinning capability and pinning force of the irradiated sample.

On the basis of these results, it can be finally said that the pinning mechanism and the superconducting properties of bulk MgB_2 superconductor can be improved by using laser irradiation in a short time.

Acknowledgments This work was supported by the Council of Higher Education (Turkey). The authors would like to acknowledge the use of Servicio General de Apoyo a la Investigación-SAI, Universidad de Zaragoza for the laser treatments. The authors gratefully acknowledge Dr. Şükrü ÇELİK (Sinop University) and S. Barış Güner (Recep Tayyip Erdogan University) for their assistance with the magnetoresistivity measurements.

References

1. J. Nagamatsu, N. Nakagawa, T. Muranaka, Y. Zentiani, J. Akimitsu, Nature **410**, 63 (2001)

2. V. Braccini, A. Gurevich, J.E. Giencke, M.C. Jewell, C.B. Eom, D.C. Larbalestier, A. Pogrebnyakov, Y. Cui, B.T. Liu, Y.F. Hu, J.M. Redwing, Q. Li, X.X. Xi, R.K. Singh, R. Gandikota, J. Kim, B. Wilkens, N. Newman, J. Rowell, B. Moeckly, V. Ferrando, C. Tarantini, D. Marré, M. Putti, C. Ferdeghini, R. Vaglio, E. Haanappel, Phys. Rev. B **71**, 012504 (2005)
3. M.H. Jung, M. Jaime, A.H. Lacerda, G.S. Boebinger, W.N. Kang, H.J. Kim, E.M. Choi, S.I. Lee, Chem. Phys. Lett. **343**, 447 (2001)
4. C. Buzea, T. Yamashita, Supercond. Sci. Technol. **14**, R115 (2001)
5. W.N. Kang, H.-J. Kim, E.-M. Choi, C.U. Jung, S.-I. Lee, Science **292**, 1521 (2001)
6. H.-J. Kim, W.N. Kang, E.-M. Choi, M.-S. Kim, K.H.P. Kim, S.-I. Lee, Phys. Rev. Lett. **87**, 087002 (2001)
7. D.C. Larbalestier, L.D. Cooley, M.O. Rikel, A.A. Polyanskii, J. Jiang, S. Patnaik, X.Y. Cai et al., Nature **410**, 186 (2001)
8. W.K. Yeoh, J.H. Kim, J. Horvat, X. Xu, M.J. Qin, S.X. Dou, C.H. Jiang, T. Nakane, H. Kumakura, P. Munroe, Supercond. Sci. Technol. **19**, 596 (2006)
9. S.X. Dou, V. Braccini, S. Soltanian, R. Klie, Y. Zhu, S. Li, X.L. Wang, D.J. Larbalestier, Appl. Phys. **96**, 7549 (2004)
10. E. Yanmaz, B. Savaskan, M. Basoglu, E.T. Koparan, N.R. Dilley, C.R.M. Grovenor, J. Alloys Compd. **480**, 203 (2009)
11. A. Serquis, X.Z. Liao, Y.T. Zhu, J.Y. Coulter, J.Y. Huang et al., J. Appl. Phys. **92**, 351 (2002)
12. S.R. Shinde, S.B. Ogale, J. Higgins, R.J. Choudhary, V.N. Kulkarni, T. Venkatesan, H. Zheng et al., Appl. Phys. Lett. **84**, 2352 (2004)
13. S. Okayasu, M. Sasase, K. Hojou, Y. Chimi, A. Iwase, H. Ikeda, R. Yoshizaki, T. Kambara, H. Sato, Y. Hamatani, A. Maeda, Phys. C **382**, 104 (2002)
14. I.M. Obaidat, H.P. Goeckner, B.A. Albiss, J.S. Kouvel, Cryst. Res. Technol. **43**, 837 (2008)
15. I.M. Obaidat, B.A. Albiss, M. Gharaibeh, M.K. Hasan, Cryst. Res. Technol. **44**, 281 (2009)
16. R.C. Ma, W.H. Song, X.B. Zhu, L. Zhang, S.M. Liu, J. Fang, J.J. Du, Y.P. Suna, C.S. Li, Z.M. Yu, Y. Feng, P.X. Zhang, Phys. C **405**, 34 (2004)
17. T.T. Palstra, B. Batlogg, L.F. Schneemeyer, J.V. Waszczak, Phys. Rev. Lett. **61**, 1662 (1988)
18. R. Griessen, Phys. Rev. Lett. **64**, 1674 (1990)
19. A.P. Malozemoff, T.K. Worthington, E. Zeldov, N.C. Yeh, M.W. McElfresh, F. Holtzberg, in *Strong Correlation and Superconductivity*, ed. by H. Fukuyama, S. Maekawa, A.P. Malozemoff (Springer, Heidelberg, 1989), p. 349
20. M. Dogruer, G. Yildirim, C. Terzioglu, J. Mater. Sci. Mater. Electron. **24**, 392 (2013)
21. X. Wan, Y. Sun, W. Song, L. Jiang, K. Wang, J. Du, Supercond. Sci. Technol. **11**, 1079 (1998)
22. M.H. Pu, W.H. Song, B. Zhao, X.C. Wu, Y.P. Sun, J.J. Du, J. Fang, Phys. C **361**, 181 (2001)
23. S. Vinu, P.M. Sarun, R. Shabna, U. Syamaprasad, J. Alloys Compd. **487**, 1 (2009)
24. O. Erdem, K. Ozturk, S.B. Guner, S. Celik, E. Yanmaz, J. Low Temp. Phys. **177**, 28 (2014)
25. M. Inui, P.B. Littlewood, S.N. Coppersmith, Phys. Rev. Lett. **63**, 2421 (1989)
26. N.V. Vo, H.K. Liu, S.X. Dou, Supercond. Sci. Technol. **9**, 104 (1996)
27. G.B. Smith, J.M. Bell, S.W. Filipczuk, C. Andrikidis, Phys. C **160**, 333 (1989)
28. J.H. Kim, S.X. Dou, D.Q. Shi, M. Rindfleisch, M. Tomsic, Supercond. Sci. Technol. **20**, 1026 (2007)
29. H. Kitaguchi, A. Matsumoto, H. Hatakeyama, H. Kumakura, Supercond. Sci. Technol. **17**, S486 (2004)
30. C.S. Yadav, P.L. Paulose, New J. Phys. **11**, 103046 (2009)
31. C.P. Bean, Phys. Rev. Lett. **8**, 250 (1962)
32. B.K. Roul, A.K. Pradhan, V.V. Rao, P. Bhattacharya, P. Pramanic, V.R. Kalvey, D.N. Bose, K.L. Chopra, Bull. Mater. Sci. **14**, 713 (1991)
33. M. Okutomi, H. Nomura, T. Tsukamoto, N.B. Dahotre, H. Shen, Nucl. Instrum. Methods Res. B **169**, 6 (2000)
34. Y. Ding, H.C. Wang, F.X. Zhao, Z.X. Shi, Z.L. Zhang, L. Ma, H.L. Suo, J. Supercond. Nov. Magn. **23**, 633 (2010)
35. P.W. Anderson, Phys. Rev. Lett. **9**, 309 (1962)
36. G. Yildirim, S. Bal, A. Varilci, J. Supercond. Nov. Magn. **25**, 1655 (2012)
37. B.K. Roul, J. Supercond. **7**, 841 (1994)
38. M. Dogruer, G. Yildirim, C. Terzioglu, J. Mater. Sci. Mater. Electron. **24**, 958 (2013)
39. D.C. Larbalestier, A. Gurevich, D.M. Feldmann, A.A. Polyanskii, Nature **414**, 368 (2001)
40. A.I. Abou-Aly, S.A. Mahmoud, R. Awad, M.M.E. Barakat, Supercond. Nov. Magn. **23**, 1575 (2010)
41. A.I. Abou-Aly, M.T. Korayem, N.G. Gomaa, R. Awad, M.A. Al-Hajji, Supercond. Sci. Technol. **12**, 147 (1999)
42. Y. Zhao, S.X. Dou, M. Ionescu, P. Munroe, Appl. Phys. Lett. **88**, 012502 (2006)
43. H.L. Li, K.Q. Ruan, S.Y. Li, Y. Yu, C.Y. Wang, L.Z. Cao, Phys. C **386**, 560 (2003)
44. S.D. Kaushik, V. Braccini, S. Patnaik, Pramana J. Phys. **71**, 1335 (2008)
45. B.K. Roul, J. Supercond. **6**, 93 (1993)
46. M.D. Sumption, M. Bhatia, S.X. Dou, M. Rindfliesch, M. Tomsic, L. Arda, M. Ozdemir, Y. Hascicek, E.W. Collings, Supercond. Sci. Technol. **17**, 1180 (2004)